(6)
A STEADY-STATE ANALYSIS OF CANDIDATE TOWING CABLES FOR A DEEP-TOWED GEOPHYSICAL ARRAY SYSTEM.

(10) Darrell A./Milburn
Martin G./Fagot

Ocean Technology Division
Ocean Science and Technology Laboratory

(11) Mar 79   (12) 37

NORDA
NAVAL OCEAN RESEARCH AND DEVELOPMENT ACTIVITY 1976

NAVAL OCEAN RESEARCH AND DEVELOPMENT ACTIVITY
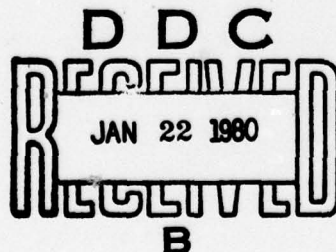NSTL STATION, MISSISSIPPI 39529   392 773

80 1 21 023

ABSTRACT

The relative performance of two candidate towing cables
for the proposed Deep-Towed Geophysical Array System is
examined. A preliminary design of this ship-towed system is
presented. It includes a description of the candidate
towing cables and a towed body, which is composed of an
instrumented fish and a long, nearly neutrally buoyant
seismic streamer.

Using a two-dimensional steady-state analysis, towing
cable geometry and tensions are predicted for the body
depths specified and for a series of towing speeds. Results
of the analysis are presented graphically and show not only
the effects of body depth and towing speed, but the effects
of cable drag coefficients and body downforce as well.
These results are then used in conjunction with constraints
on cable length and design tension to predict maximum towing
speeds.

Although based on a particular design, the information
contained in this report provides useful guidance to further
assist in the engineering development of the overall system.

CONTENTS

ILLUSTRATIONS

TABLES

NOTATION

A	Area of towed body component
C_D	Drag coefficient of towed body component
C_n	Normal drag coefficient of towing cable
C_t	Tangential drag coefficient of towing cable
d	Cable diameter
D	Drag force on the towed body
D_i	Drag force on i th component of the towed body
f_n	Hydrodynamic force per unit length normal to the cable
f_t	Hydrodynamic force per unit length tangential to the cable
H	Depth of fish and seismic streamer
L	Length of towing cable used to tow body at depth H
L_{max}	Maximum length of towing cable available
s	Distance along the towing cable
SF	Safety factor
T	Cable tension
T_1	Cable tension at the fish (s = 0)
T_2	Cable tension at the ship (s = L)
T_{max}	Design tension for towing cable
V	Towing speed
V_C	Ocean current speed, uniform with depth
V_n	Flow velocity normal to the cable
V_R	Relative flow speed equal to V plus V_C
V_t	Flow velocity tangential to the cable
w	Weight per unit length of towing cable in water
W_f	Weight in water of the fish or body downforce
$W_f^{(k)}$	k th value of W_f
x,y	Cartesian coordinates

$\bar{x}$ Trail (horizontal distance of the fish behind the ship)

γ	(gamma)	
γ_1		Normal drag amplification factor
γ_2		Tangential drag amplification factor
ϵ	(epsilon)	Error term
$\epsilon^{(k)}$		kth value of ϵ
ρ	(rho)	Mass density of sea water
ϕ	(phi)	Angle between the flow velocity and the cable tangent
ϕ_1		Value of ϕ at $s = 0$
ϕ_2		Value of ϕ at $s = L$

I. INTRODUCTION

The Geophysical Array is a ship-towed system being developed to accurately measure, in deep water, various geophysical properties of the ocean floor and subbottom structure (Fagot and Eckstein, 1979). The design concept is shown schematically in Figure 1 where the basic system components identified are a ship, a towing cable, and a towed body. As shown, the towed body is composed of a fish that contains an acoustic sound source and a long seismic streamer that contains hydrophones and engineering sensors.

To achieve the deep body depths shown in Figure 1, it is necessary to use a long length of towing cable. Because of this, towing speed is an important performance criterion. For example, if speeds are too low the ship will have difficulty towing in a steady, straight course. As is known, departures in speed and course can impart motions to the seismic streamer which, in turn, can degrade the geophysical measurements. Since a ship generally has better sea-keeping ability at higher speeds, it is therefore desirable to maximize towing speed within the limits of cable design tension.

To achieve maximum speed for a specified body depth, it is axiomatic that drag must be minimized and downward forces maximized. The best manner of minimizing cable drag is to reduce cable size and to use cable fairings. Downward forces can be maximized by increasing cable weight and depression force acting on the towed body. In selecting the optimum cable design, however, other cable characteristics must be considered. These characteristics, critical to system survival, include: Corrosion and abrasion resistance, torsional behavior, and fatigue life, to name a few.

In this report, the relative performance of two candidate towing cables is examined. Using a well-established, two-dimensional, steady-state analysis (adequate for a preliminary design), towing cable geometry and tensions are predicted for the two body depths shown in Figure 1 and for a series of towing speeds. Results of the analysis are presented graphically and show not only the effects of body depth and towing speed, but the effects of cable drag coefficients and body downforce as well. These results are then used in conjunction with constraints on cable length and design tension to predict maximum towing speeds.

Although based on a particular system design, the information contained herein provides useful guidance to further assist in the engineering development of the overall system.

II. ANALYTICAL MODEL

A. DIFFERENTIAL EQUATIONS OF EQUILIBRIUM

The two-dimensional model used in this study is based on a well-established theory of cables subjected to a relative flow. It assumes that all forces and the cable are coplanar and that the relative flow is constant and uniform with depth. It further assumes that the towing cable is inextensible and offers no resistance to bending. Also, the hydrodynamic forces acting on an element of cable are assumed to be a function of cable angle only.

Figure 2 shows schematically the equilibrium configuration of the Geophysical Array System with respect to a Cartesian coordinate system (x,y) used in this study. The directions of the system, whose origin is located at the point
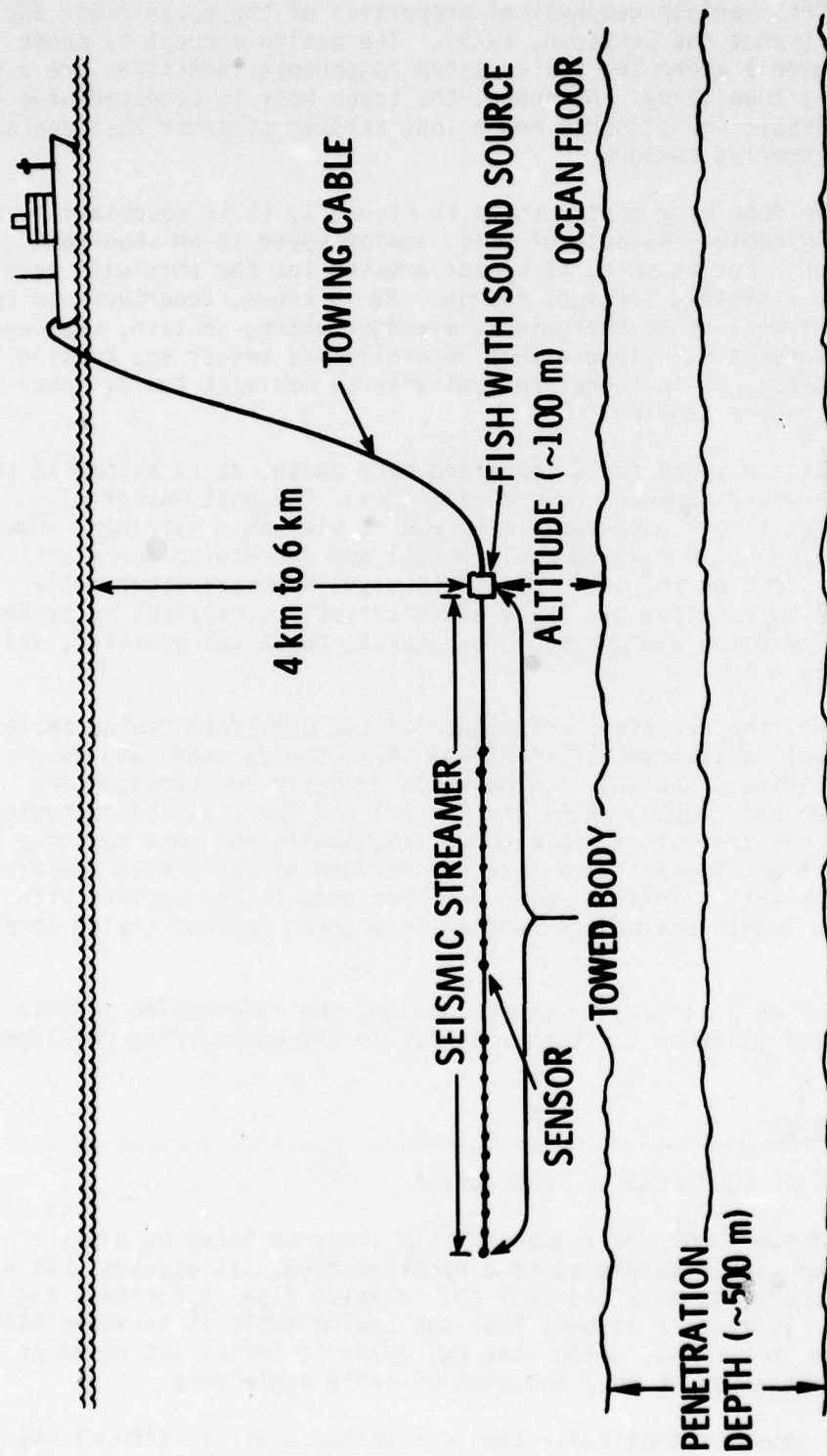
1

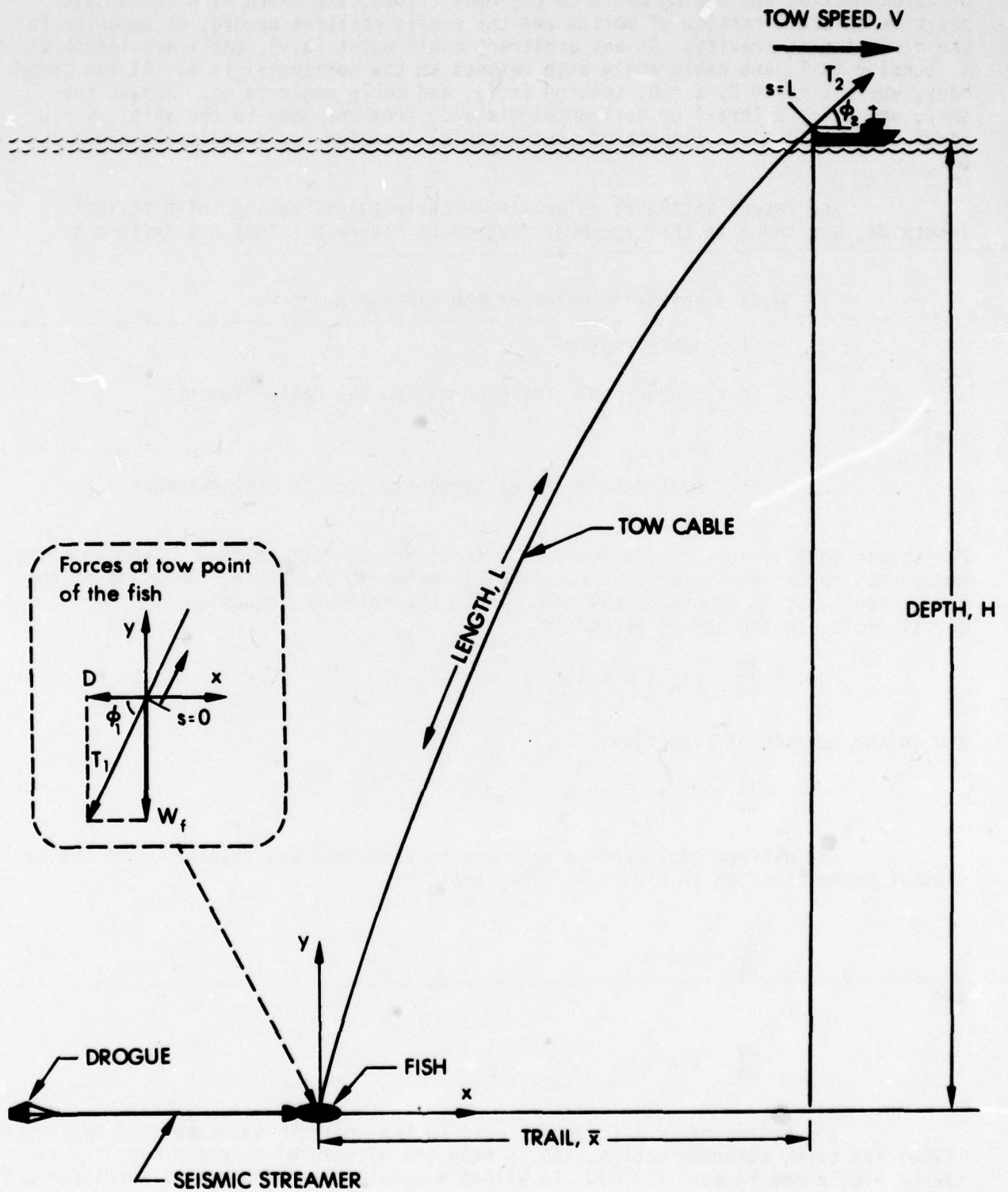Figure 1. Design concept of the Deep-Towed Geophysical Array System

Figure 2. Schematic diagram of the equilibrium configuration of the towed system

of attachment of the towing cable to the body (fish), are fixed with the x-axis positive in the direction of motion and the y-axis positive upward, or opposite to the direction of gravity. At any arbitrary cable point (x,y), cable arc length is s, tension is T, and cable angle with respect to the horizontal is ϕ. At the towed body, where $x = y = 0$, $s = 0$, tension is T_1, and cable angle is ϕ_1. And at the ship, where $x = \bar{x}$ (trail or horizontal distance from the body to the ship), $y = H$ (body depth) and $s = L$ (length of towing cable), tension is T_2 and cable angle is ϕ_2.

The forces acting at an arbitrary cable point, having infinitesimal length ds, are shown in the free-body diagram of Figure 3. They are defined as

w ds = weight in water of the cable element

T = cable tension

f_n ds = hydrodynamic force normal to the cable element

and

f_t ds = hydrodynamic force tangential to the cable element

For static equilibrium, the vector sum of these forces must be zero. Summing force components normal and tangential to the cable element, and taking the limit of the force resultants as ds approaches zero, yield the following equations of equilibrium: In the normal direction

$$T \frac{d\phi}{ds} = -f_n + w \cos \phi \tag{1}$$

and in the tangential direction

$$\frac{dT}{ds} = f_t + w \sin \phi \tag{2}$$

The differential cable displacements equations are obtained from the cable element geometry shown in Figure 3. They are:

$$\frac{dx}{ds} = \cos \phi \tag{3}$$

and

$$\frac{dy}{ds} = \sin \phi \tag{4}$$

The hydrodynamic force model used in the analysis was developed by Wilson (1960) for bare, stranded cables, and is only one of several proposed over the years, see Casarella and Parsons (1970). In Wilson's model, the hydrodynamic force per unit length acting normal to the cable is defined as

$$f_n = \tfrac{1}{2}\rho \, C_n \, d \, V_n^2 \; = \tfrac{1}{2}\rho \, C_n \, d \, V^2 \sin^2 \phi \quad , \tag{5a}$$
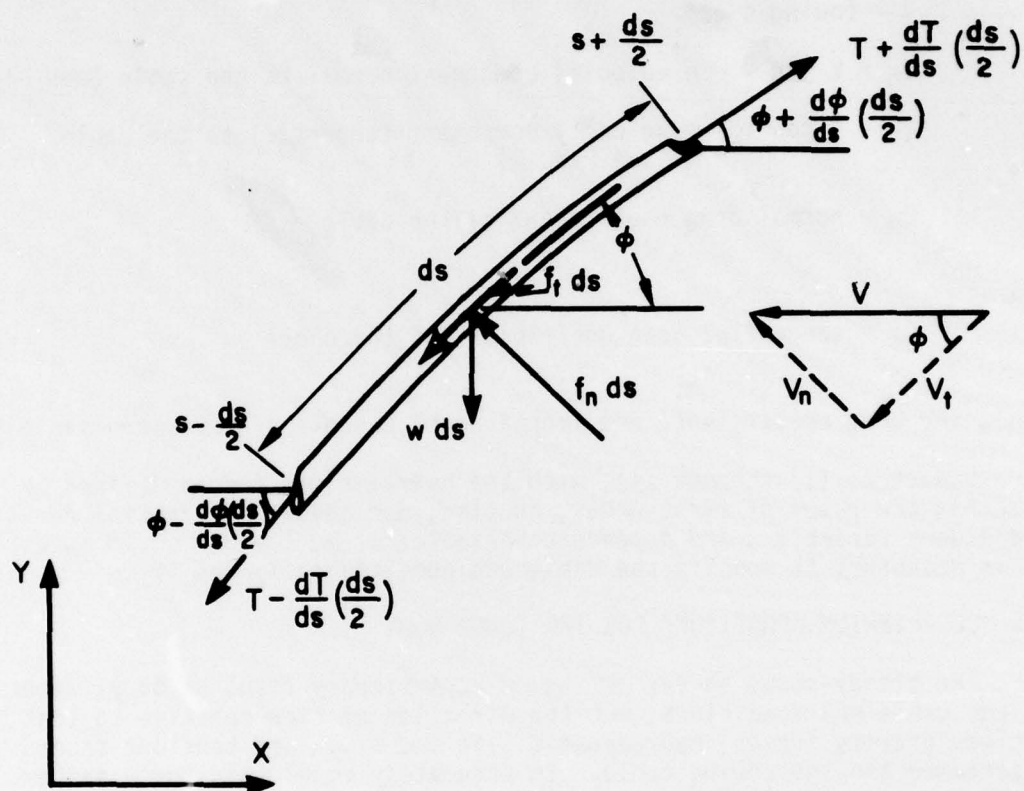
4

Figure 3. Free-body diagram of a differential cable element

5

and the hydrodynamic force per unit length tangential to the cable as

$$f_t = \tfrac{1}{2}\rho \, C_t(\pi d)V_t^2 = \tfrac{1}{2}\rho \, C_t(\pi d)V^2 \cos^2 \phi \tag{5b}$$

where

ρ = mass density of fluid

d = cable diameter

V = towing speed

$V_n = V \sin \phi$ = velocity component normal to the cable (see Fig. 3)

$V_t = V \cos \phi$ = velocity component tangential to the cable (see Fig. 3)

C_n = normal drag coefficient of the cable

and

C_t = tangential drag coefficient of the cable

In general, the drag coefficients are functions of Reynold's number and cable type.

Equations (1) through (4), with the hydrodynamic forces defined by Equations (5), are a set of first-order, coupled, nonlinear differential equations with independent variable s and dependent variables x, y, T and ϕ. To integrate them, it is necessary to specify the cable end conditions: T_1 and ϕ_1.

B. EQUILIBRIUM CONDITIONS FOR THE TOWED BODY

The steady-state forces acting on an arbitrary fish, or body, determine not only the cable end conditions, but the direction of flow relative to that body. These include gravity forces, hydrodynamic lift and drag, and tensions caused by the seismic streamer and the towing cable. To accurately model this force system, a detailed body design (including an accurate description of the variation of hydrodynamic forces with pitch angle) is required. However, this accuracy is not presently needed, since this is a first approximation design study.

To simplify the analysis, the force system shown in the free-body diagram of Figure 2 is assumed to approximate the more general force system described above. The forces shown acting at the cable end s = 0 are: A body downforce, W_f, caused by gravity forces and possibly a speed-dependent depressing force, and a drag force, D, which acts in the direction of relative flow. Applying the equations of equilibrium to this concurrent force system then gives the cable end conditions as

$$T_1 = (W_f^2 + D^2)^{\tfrac{1}{2}}$$

and

$$\phi_1 = \tan^{-1} (W_f/D)$$

6

To calculate the drag force, it is reasonable to assume that

$$D = \sum_{i=1}^{n} D_i$$

where n is the number of towed body components and D_i is the drag on the i th component. Substituting the formula

$$D_i = \tfrac{1}{2} \rho \ (C_D A)_i \ V^2$$

into the above equation, then gives the desired expression as

$$D = \tfrac{1}{2} \rho V^2 \sum_{i=1}^{n} (C_D A)_i \tag{6}$$

where C_D is the drag coefficient and A is the area, viewed in the direction of V.

Thus, the towed body characteristics, $(C_D A)_i$ and W_f, determine the initial conditions for the cable.

III. THE TOWED SYSTEM: A PRELIMINARY DESIGN

A. CANDIDATE TOWING CABLES

Based on some electrical and nonelectrical design considerations, two cables having identical diameters (1.75 cm) were selected for the analysis. Each cable is a coaxial-type construction having two contrahelically wound layers of galvanized, high-strength steel wires wrapped around an electrical core. To reduce torsional response, the layers of each cable are reversed-wrapped: the inner layer in a right-hand lay, the outer layer in a left-hand lay. The electrical cores, which are adequate for the data transmission and powering schemes presently under consideration, have about the same diameters and electrical characteristics.

The two cables, however, have different mechanical characteristics which are related to differences in wire geometry (e.g., pitch diameter and helix angle) and the amount of metallic, load-bearing area. For purposes of discussion, the cable with the least amount of load-bearing area will be referred to as Cable I and the one with the greatest amount as Cable II.

Cable I, designed for a particular towing application, is shown in Figure 4. Its inner layer contains 16 wires, its outer layer 18 wires. As shown, the adjacent wires in each layer are not in contact, but instead are spaced apart to reduce torque. To provide abrasion and corrosion resistance, the cable is covered with a hytrel jacket. In contrast, Cable II (a standard catalog cable design) has no protective jacket. Also, it has more wires in each layer and each of these wires has a greater diameter than those of Cable I. Therefore, Cable II, whose adjacent wires are not spaced apart, has more load-bearing area than does Cable I. Because of its greater load-bearing area, Cable II has a greater breaking strength and unit weight in water than does Cable I: 142.3 kN compared to 90.7 kN and 7.29 N/m compared to

7
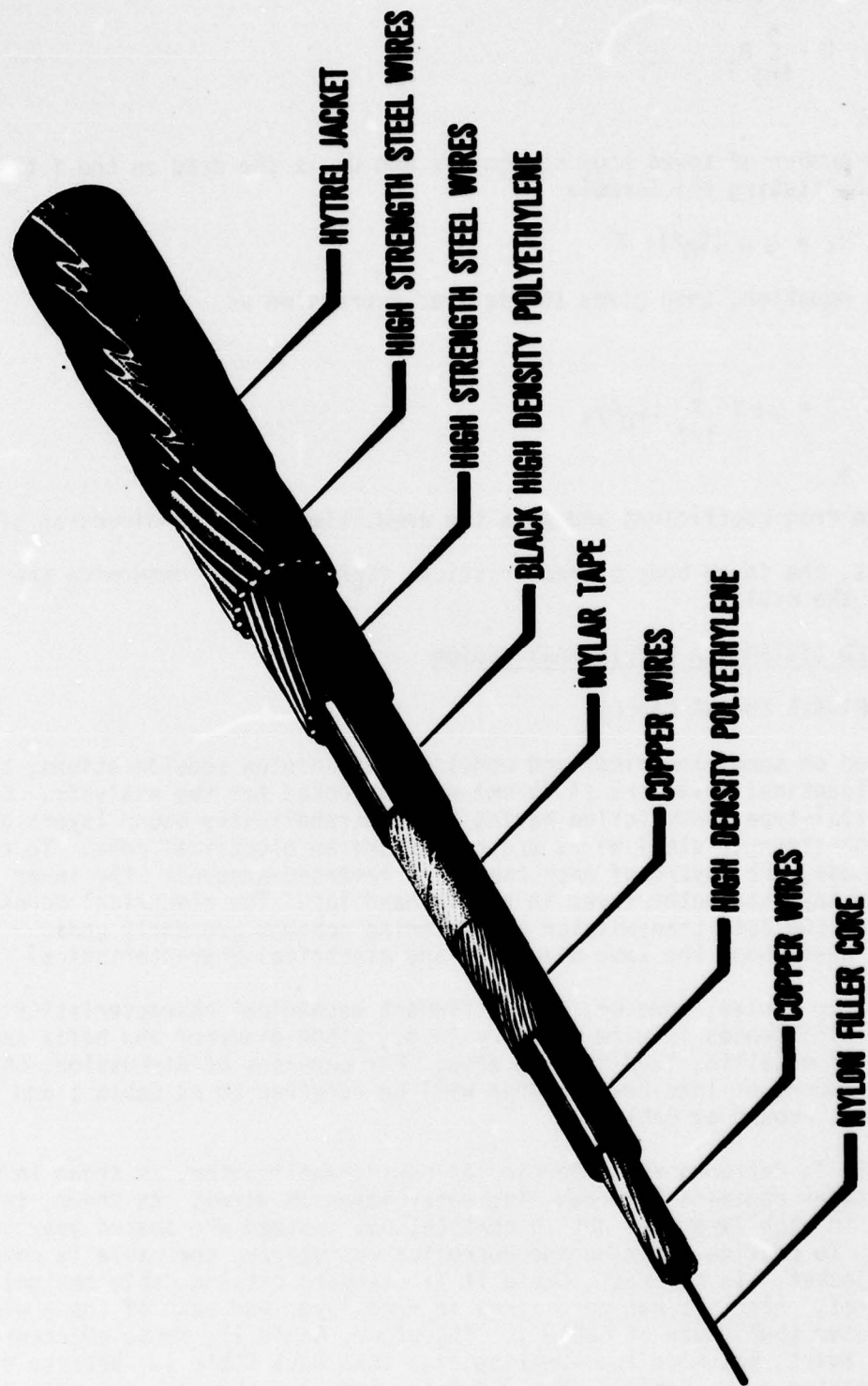
Figure 4. Cable I: A double armored, steel, coaxial cable

HYTREL JACKET

HIGH STRENGTH STEEL WIRES

HIGH STRENGTH STEEL WIRES

BLACK HIGH DENSITY POLYETHYLENE

MYLAR TAPE

COPPER WIRES

HIGH DENSITY POLYETHYLENE

COPPER WIRES

NYLON FILLER CORE

5.02 N/m.   And therefore, the analysis will show that Cable II performs better than Cable I.

However, in selecting the optimum cable design, other mechanical characteristics not used in the steady-state analysis must be evaluated and weighted in terms of their importance. Some of these include corrosion and abrasion resistance, torsional behavior, and fatigue life. Since Cable I is better than Cable II in regard to these characteristics, it was also deemed a candidate for analysis.

B. SELECTION OF CABLE DRAG COEFFICIENTS

The values of drag coefficients, C_n and C_t, selected for the candidate towing cables are based on the results of Wilson (1960) and on a factor that is intended to account for cable strumming. Wilson, who analyzed the experimental data of others, concluded that the drag coefficients for bare, stranded cables are approximately constant, and within a practical working range, are independent of Reynold's number. In particular, he recommends a normal drag coefficient of 1.4 and tangential drag coefficients ranging from 0.004 to 0.014.

But Wilson's data do not account for strumming caused by vortex shedding. As is well known (Griffin et al., 1975), strumming leads to a virtual increase of the steady-state drag coefficient over that value measured for a stationary, or nonstrumming, cable. To calculate these virtual drag coefficients, the following formulas are used:

$$C_n = 1.4 \, \gamma_1 \tag{7a}$$

and

$$C_t = a \, \gamma_2, \quad 0.004 \leq a \leq 0.014 \tag{7b}$$

where γ_1 and γ_2 are drag amplification factors that depend on the strumming behavior of the cables. Although limited, data are available in the literature for estimating appropriate values of γ_1, but not for γ_2.

The most recent and pertinent data are those given by Skop et al. (1976) and by Casarella and Parsons (1970). Using their recently developed strumming modeling techniques, Skop et al. investigated the strumming behavior of a particular delta-shaped cable array. An examination of their results shows that values of γ_1 can range from 1.3 to 2.3 for the stranded cables comprising the delta. Casarella and Parsons report results which also show that a drag increase of about 35% can be experienced, $\gamma_1 = 1.35$. For lack of information regarding values of γ_2, it appears reasonable to take $\gamma_2 = \gamma_1$.

Based on Equations (7) and the range of values given above for γ_1, three sets of drag coefficients have been selected for the analysis. They are

$$C_n = 1.4 \text{ and } C_t = 0.0$$

$$C_n = 1.8 \text{ and } C_t = 0.006$$

and

$$C_n = 2.7 \text{ and } C_t = 0.02$$

9

The first set assumes no strumming ($\gamma_1 = 1.0$) and no tangential drag (a = 0), and therefore has the lowest values to be expected. The second set, however, assumes a reasonable amount of strumming ($\gamma_1 = \gamma_2 = 1.29$, a = 0.005) and appears to be the most realistic of the three sets. And the third set assumes a considerable amount of strumming ($\gamma_1 = \gamma_2 = 1.9$, a = 0.01) and possibly has the highest expected values. This judicious selection is intended to show the effects of changes in drag coefficient values as well as to provide probable bounds on several computed parameters.

C. TOWED BODY CHARACTERISTICS

The essential characteristics of the fish and seismic streamer, the basic parts of the towed body, are tabulated in Table 1. These characteristics include values of C_DA, drag force, and weight in water for the components listed as well as values of D and W_f. It can be seen that the fish accounts for 32% of D and all of W_f, and that the seismic streamer accounts for 68% of D and none of W_f.

The fish, designed to house an instrument payload, is a framed structure 1.1 m high by 0.9 m wide by 1.5 m long. Its C_D is 1.0 (Hoerner, 1965) and its area is about 1 m^2. It is a wingless body that generates downforce, not by hydrodynamic flow but by means of its own weight. When fully flooded, it weighs 5.3 kN in water. Additional downforce can be obtained, however, by adding "dead weight," wings, or a combination of both.

The seismic streamer, consisting of an array section, a tail, and a drogue, is 1050 m long and has varying degrees of buoyancy along its length. The array section, 550 m long and located at the upstream-end of the seismic streamer, is a free-flooded, Kevlar, electromechanical cable having 12 hydrophones and four depth sensors. The hydrophones, which are spread over a 500 m acoustic aperture, and the depth sensors are mounted coaxially in the array cable by a technique described by Milburn and Rumpf (1979), see Figure 6. The array cable has a 3.2 cm diameter and, not including the sensors, is negatively buoyant 2.3 N/m. The tail, 500 m long and located aft of the array section, is a rope having a 3.2 cm diameter and is neutrally buoyant. The drogue is located at the downstream-end of the seismic streamer and, like the tail, provides additional tension to minimize deformations in the acoustic aperture of the array. The size, shape and weight estimates for the sensors and drogue are given in Figure 5.

Because the array section is negatively buoyant, it is rendered neutrally buoyant (approximately) by judiciously distributing 33 syntactic foam floats along the seismic streamer. Figure 5 gives the characteristics of these floats and Figure 6 shows one attached to a piece of array cable.

IV.   PERFORMANCE PREDICTION

A. CASES INVESTIGATED

Two types of problems are investigated, an initial-value problem and a boundary-value problem. For each type, 12 cases derived from the combinations of the two towing cables, three sets of cable drag coefficients, and two towing depths (4 km and 6 km) are analyzed. Each case can be seen in Table 2 where characteristics applicable to the analysis are given.

The fish described in Section III-C is referred to as the initial body design. When dead weight or wings are added to it, a new body design having increased downforce, and possibly drag, is obtained. As shown in Table 2, the

TABLE 1

LIST OF TOWED BODY COMPONENTS AND THEIR CHARACTERISTICS

Component	$\sum_{i=1}^{n} (C_D A)_i$ (m^2)	$\left(\sum_{i=1}^{n} D_i\right)^a$ (N)	Weight in water of n components[b] (kN)
• Fish, n=1	1.0	511 V^2	-5.3
• Seismic streamer			
Array cable, n=1	0.44[c]	226 V^2	-1.3
Tail, n=1	0.40[c]	205 V^2	0.0
16 sensors, 33 floats, and a drogue, n=50	1.28[d]	653 V^2	+1.3
TOTALS		D = 1595 V^2	W$_f$ = -5.3

[a]D_i and D, computed from Eq. (6), are in newtons for V in m/s.

[b]Weight is used to mean force of gravity, and therefore is measured in newtons. Also, a minus sign indicates negative buoyancy and a plus sign positive buoyancy.

[c]$A = \pi$ x diameter x length and $C_D = 0.008$, Wilson (1960).

[d]Values of A and C_D are given in Fig. 5 for each component.

TABLE 2

CASES INVESTIGATED

	Cable I	Cable II
● Cables:		
Diameter, d (cm)	1.75	1.75
Weight in water, w (N/m)	5.02	7.29
Breaking strength, BS (kN)	90.7	142.0
Drag coefficients[a]	I, II, and III	I, II, and III

● Towed body:

Drag, $D = 2393 \, V^2$ in newtons for V in m/s

Downforce, $W_f = 5.3$ kN for the initial-value problems and
$W_f \geq 5.3$ kN for the boundary-value problems

● Water depths: H = 4 km and 6 km

---

[a] Drag coefficient sets - I: $C_n = 1.4$ and $C_t = 0.0$

II: $C_n = 1.8$ and $C_t = 0.006$

III: $C_n = 2.7$ and $C_t = 0.02$

(a) Hydrophone or depth sensor housing

0.6m

8cm

V

Shape: Cone

A = 5.0 x 10⁻³ m²
Re = 1.3 x 10⁴ — 8 x 10⁴
C_D = 0.1
Weight in water = -9.3 N

(b) In-line float

0.46m

0.23m

V

Shape: Prolate spheroid

A = 4.2 x 10⁻² m²
Re = 4 x 10⁴ — 2 x 10⁵
C_D = 0.27
Weight in water = +43.6 N

(c) Drogue assembly

SMALL SWIVEL

TAIL

0.9m

V

DROGUE

ONE OF FOUR
WIRE SUPPORTS

Shape: Frustrum of a cone

A = 0.64 m²
Re = 1.5 x 10⁵ to 9 x 10⁵
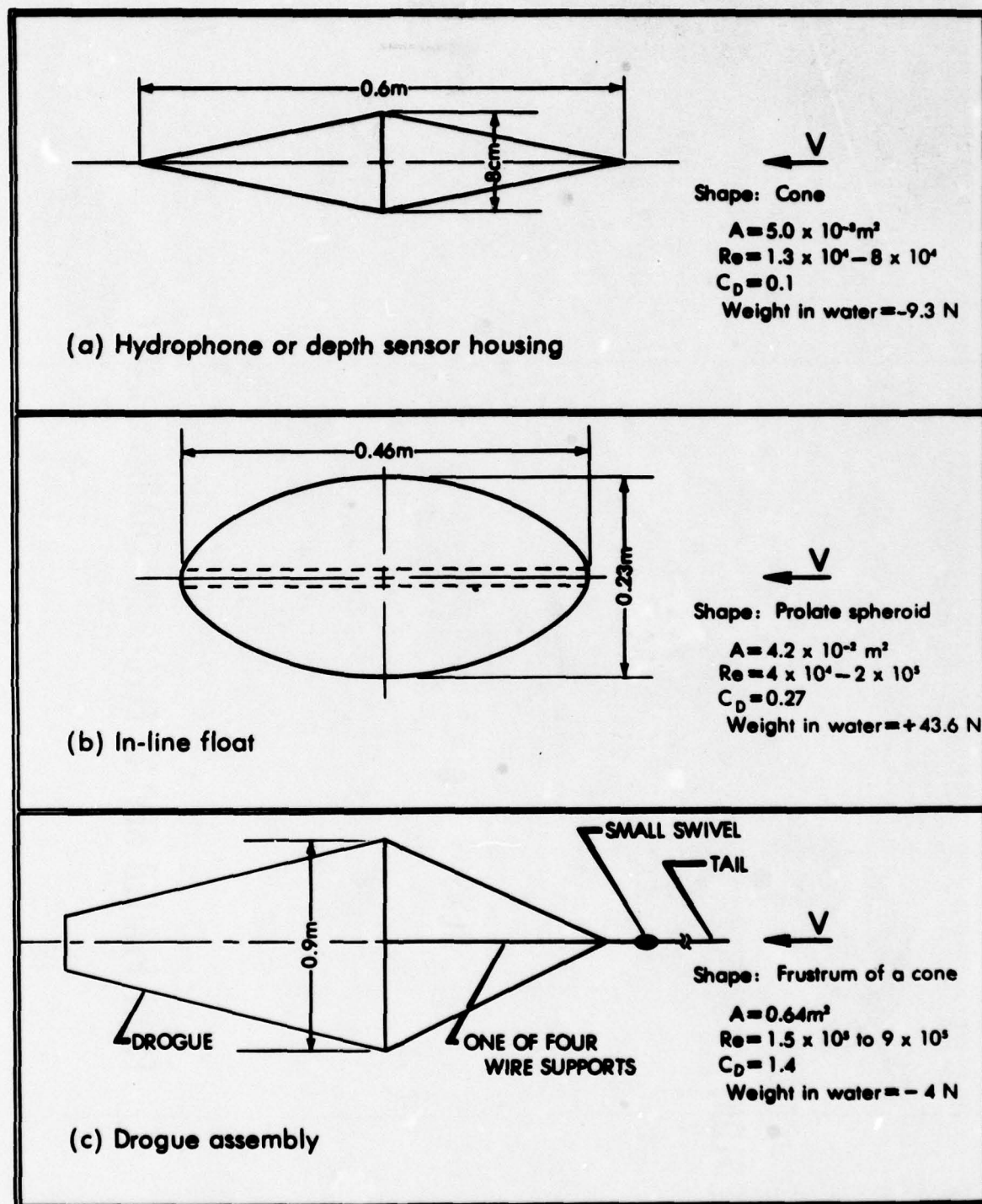C_D = 1.4
Weight in water = - 4 N

Figure 5. Schematic drawing of some seismic streamer components (the drag coefficient values shown are from Pattison, 1977)

IN-LINE FLOAT

SENSOR STATION

EIGHT PLAITED KEVLAR ELECTROMECHANICAL CABLE

initial-value problems consider the initial body design having $W_f = 5.3$ kN and the boundary-value problems new body designs having $W_f \geq 5.3$ kN. The body drag for the new body designs is assumed to be the same as that for the initial body. This is a reasonable assumption, since adding weight to the initial body will not necessarily affect its overall size and shape. But if wings are added to the initial body design drag will generally be increased. To account for any increase and to be conservative, the drag expression given in Table 1 for the initial body design is increased by 50% as shown in Table 2.

For a given towing speed, the solution of the initial-value problems is straightforward. In particular., the integration of the differential equations (by a fourth-order, Runge-Kutta method) begins at $s = 0$ where the dependent variables are known, or computed, as

$$x = y = 0$$

$$T_1 = (D^2 + W_f^2)^{\frac{1}{2}} \tag{8}$$

$$\phi_1 = \tan^{-1}(W_f/D)$$

and proceeds until $y = H$. This procedure is then repeated for a series of increasing towing speeds.

As speed is increased, the cable lengths required to tow at the specified depth and the cable tensions will also increase. But a speed is reached when values of either L or T_2 become too great. This speed is a maximum for the towed system having the initial body design and is defined when $L = L_{max}$ (maximum cable length available) or $T_2 = T_{max}$ (design tension). The maximum cable length, which is important from operational, cost, and reliability viewpoints, is assumed to be 9.15 km. The design tension, which is important to an assessment of system survival, is defined as

$$T_{max} = BS/SF$$

where BS is the breaking strength of the towing cable and SF is an appropriate safety factor. Although it is common practice to use a safety factor of three, results for safety factors as low as two are considered in the analysis.

In computing the initial-value problems, it was found that L_{max} was reached before T_{max}. Since T_2 is less than T_{max}, it is possible to achieve speeds greater than those with the initial body design by considering body designs with $W_f > 5.3$ kN. To compute the maximum speeds for these new body designs, the solution of a boundary-value problem is required. In this formulation, the differential equations are solved in conjunction with the following boundary conditions:

At $s = 0$

$$x = y = 0$$

$$D = 2393 \ V^2 \tag{9a}$$

and at $s = L_{max} = 9.15$ km

$$y = H \tag{9b}$$

B. SOLUTION METHOD FOR THE BOUNDARY-VALUE PROBLEMS

The method used to solve the boundary-value problems is an iterative procedure that automatically adjusts guesses of W_f by solving a series of initial-value problems. For a particular towing speed, an assumed value, or guess, of W_f establishes the initial conditions for the differential equations, see Equation (8). But if the guess is incorrect, then the depth predicted by integrating the differential equations from $s = 0$ to $s = L_{max}$ will be wrong. This is illustrated in Figure 7(a) where two hypothetical cable configurations are shown. The configuration denoted by the solid curve represents the exact solution, or correct value of W_f, and is therefore shown to satisfy the boundary condition on depth. The other configuration is based on an arbitrary, but incorrect, value of W_f and is therefore shown to miss the boundary condition on depth by an amount, ε, where

$$\varepsilon = H - y\big|_{s = L} \tag{10}$$

To adjust the incorrect value of W_f, the following iterative formula based on Newton's method is applied

$$W_f^{(k+1)} = W_f^{(k)} - \left[\varepsilon \left(\frac{d\varepsilon}{dW_f}\right)^{-1} \right]^{(k)} , \quad k \geq 1 \tag{11a}$$

where the superscript notation denotes values for each iteration, e.g., k=1 is the first iteration; k=2, the second; and so on. Because the derivative in Equation (11a) cannot be expressed functionally, it is approximated by placing a straight line through two successive points as shown in Figure 7(b). And as a general formula, it can be written as

$$\left(\frac{d\varepsilon}{dW_f}\right)^{(k)} \approx \frac{\varepsilon^{(k-1)} - \varepsilon^{(k)}}{W_f^{(k-1)} - W_f^{(k)}} , \quad k \geq 2 \tag{11b}$$

Substituting Equation (11b) into Equation (11a) then gives the desired recursion formula as

$$W_f^{(k)} = W_f^{(k-1)} - \varepsilon^{(k-1)} \left[\frac{W_f^{(k-2)} - W_f^{(k-1)}}{\varepsilon^{(k-2)} - \varepsilon^{(k-1)}} \right] , \quad k \geq 3 \tag{11c}$$

An inspection of Equation (11c) shows that values of $W_f^{(1)}$ and $W_f^{(2)}$ are required to start the iterative procedure. After estimating these values, the differential equations are integrated and values of $\varepsilon^{(1)}$ and $\varepsilon^{(2)}$ are computed from Equation (10). Next, an adjusted value, $W_f^{(3)}$, is found from Equation (11c). The procedure is then repeated until the error, $\varepsilon^{(k)}$, becomes as small as desired.

For the computations made in this study, convergence (i.e., ε approaching zero) was always obtained, and usually after six integrations of differential equations.
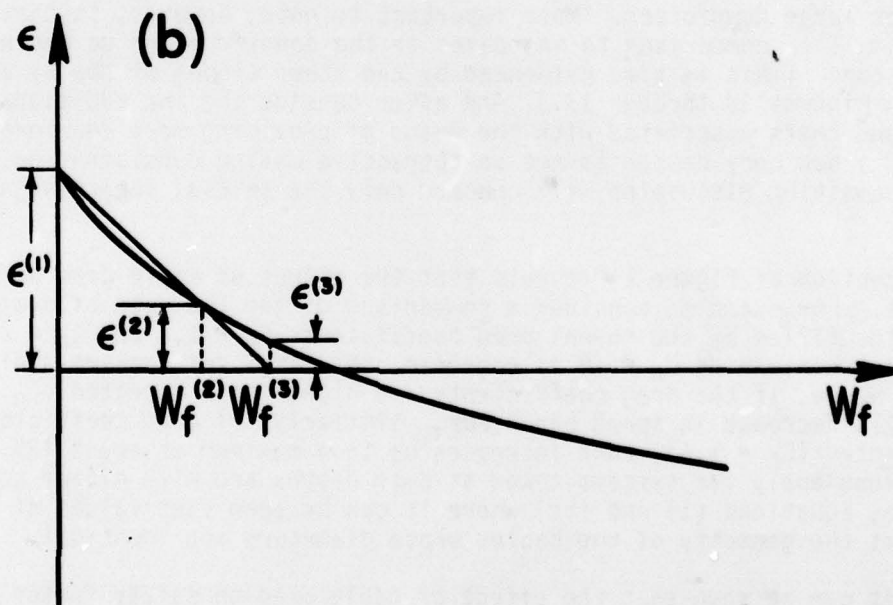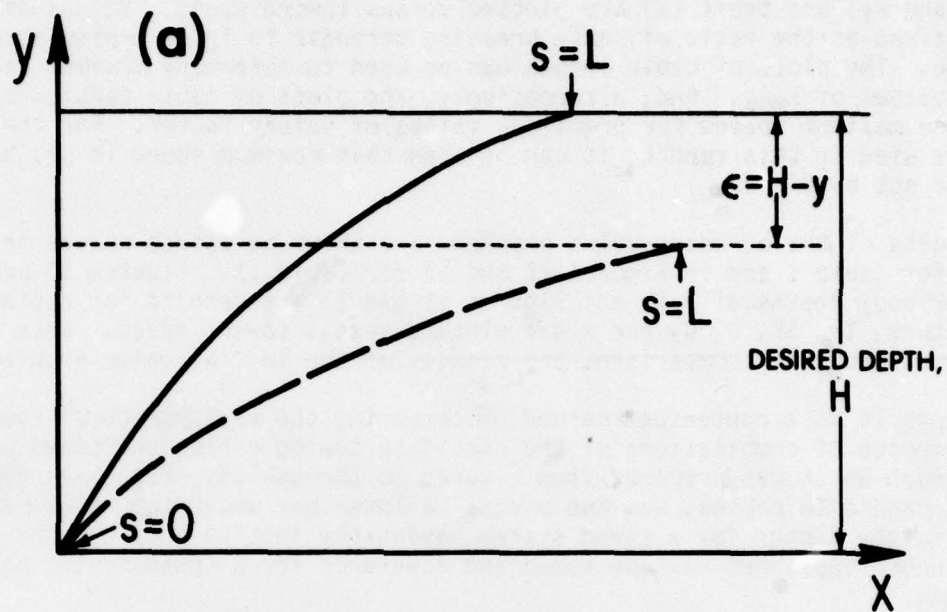
16

Figure 7. Schematic diagram showing solution technique for the boundary-value problem: (a) Error, ε; (b) Generalized Newton's method.

17

V.   DISCUSSION OF RESULTS

The results of the initial-value problems are shown in Figure 8 for Cable I and in Figure 9 for Cable II. In each figure, cable length (L), tension (T_2), body forces (D and W_f) and trail (x) are plotted versus towing speed. Values of safety factor, defined as the ratio of cable breaking strength to T_2, are also shown for convenience. The plots of cable length can be used to determine maximum speeds for practical values of L_{max}. And, alternatively, the plots of cable tension can be used to determine maximum speeds for practical values of safety factor. For the constraints used in this report, it can be seen that maximum speed is set by L_{max} = 9.15 km and not by SF = 2.

Results of the boundary-value problems are shown by dashed curves in Figures 10 and 11 for Cable I and in Figures 12 and 13 for Cable II. Figures 10 and 12 are results for body depths of 6 km and Figures 11 and 13 are results for depths of 4 km. In each figure, T_2, SF, D, W_f and x are plotted versus towing speed. Note that the solid curves, shown for comparison, are results of the initial-value problems.

Figure 14 is a convenient method of comparing the performance of towed system designs composed of combinations of the candidate towing cables and towed bodies. It is a bar graph which was prepared from Figures 10 through 13. Each bar, representing one of the candidate cables, has two parts: A lower bar whose top shows maximum speed and safety factor for a towed system having the initial body design; and an upper bar whose top shows maximum speed and downforce for a towed system having a new body design.

Referring to the upper bars, it can be seen that the maximization of speed requires rather large downforces. More important to note, however, is that increases in speed are small in comparison to increases in the downforce and to decreases in the safety factor. (This is also evidenced by the steep slopes of the W_f and T_2 plots shown in Figures 10 through 13.) And after considering the additional handling difficulties and costs associated with the means of providing more downforce, it is concluded that a new body design is not an attractive design consideration. Because of this, the remaining discussion will concern only the initial body design, or lower bars.

An inspection of Figure 14 reveals that the effect of cable drag on speed can be significant. For example, consider a comparison of the two sets of drag coefficients identified by the normal drag coefficients C_n = 1.8 and C_n = 2.7. Although the set containing C_n =1.8 is expected, the other set remains a distinct possibility. Hence, if the drag coefficients are higher than expected (C_n = 2.7), then about a 17% decrease in speed can occur. Similarly, if drag coefficients are less than expected (C_n = 1.4), then increases up to a maximum of about 13% can occur. These comparisons apply for systems towed at both depths and with either cable. This is explained by Equations (1) and (5a) where it can be seen that values of C_n strongly affect the geometry of the cables whose diameters are identical.

Also, it can be seen that the effect of cable drag on safety factor is negligible for towing the initial body with either cable at H = 6 km and is small at H = 4 km. This is a result of cable weight and body forces being much larger than tangential cable drag caused by values of C_t, see Equations (2) and (5b). Therefore, it is more important to reduce values of C_n, possibly by using flexible fairing, than it is to reduce values of C_t.

For purposes of comparison, the bars representing cables with identical drag coefficients are shown adjacent to one another in Figure 14. As can be seen, Cable
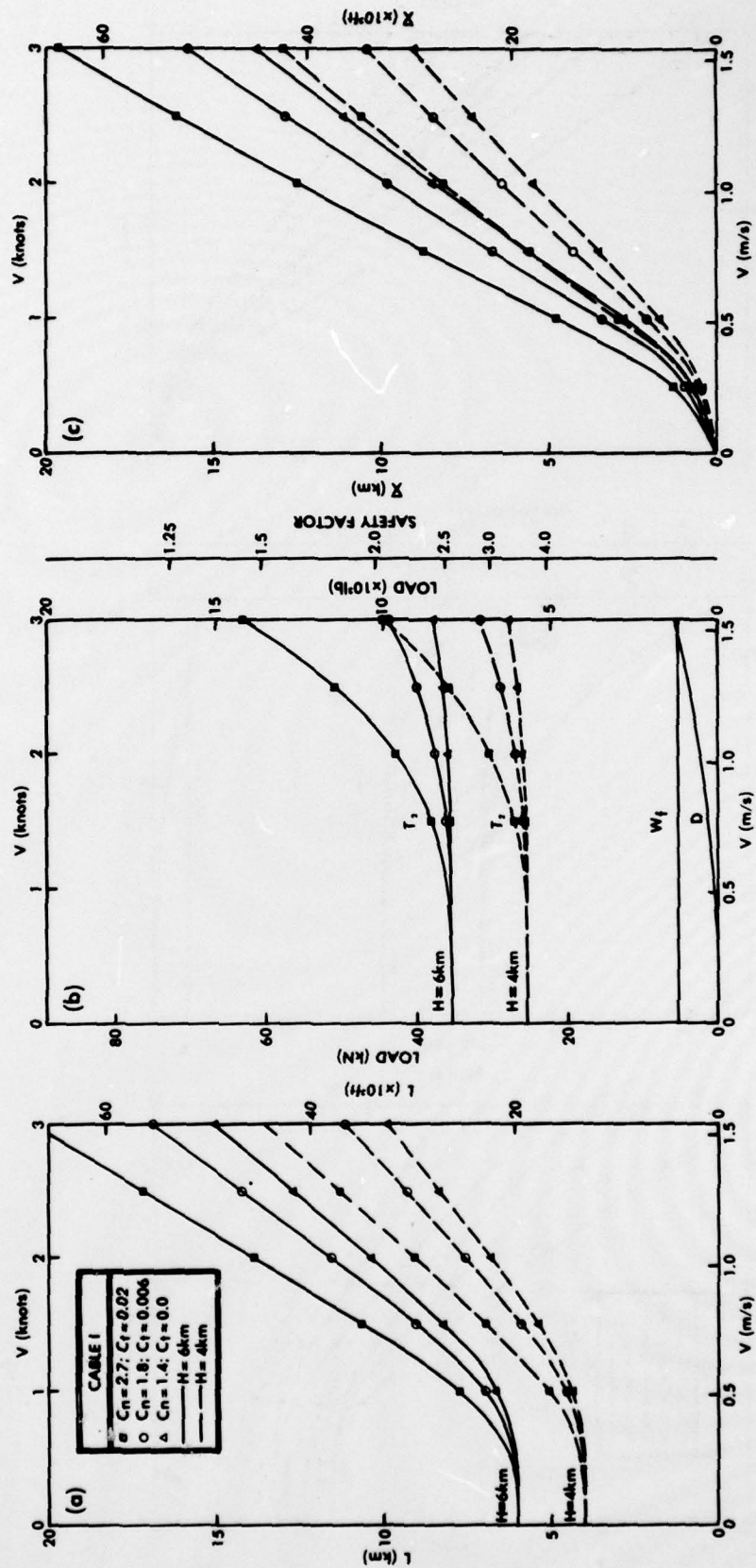
18

Figure 8. Cable I -- Effect of towing speed, depth and drag coefficients on cable
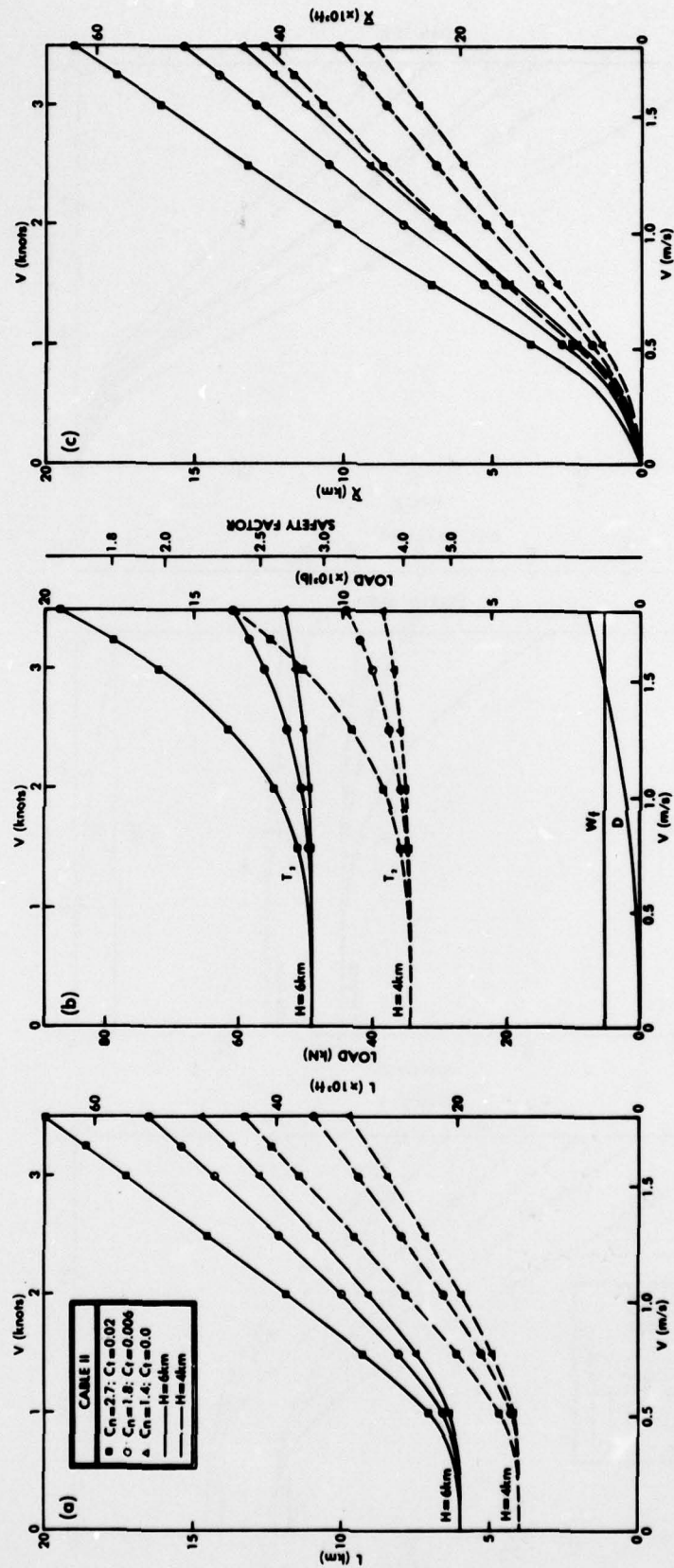length, loads, and trail: (a) L vs. V; (b) T_2, W_f, and D vs. V;
(c) $\bar{x}$ vs. V

Figure 9. Cable II -- Effect of towing speed, depth and drag coefficients on cable length, loads, and trail: (a) L vs. V; (b) T_2, W_f, and D vs. V; (c) $\bar{x}$ vs. V

Figure 10. Cable I -- Effect of towing speed and drag coefficients on loads and trail for H = 6 km: (a) T_2, W_f, and D vs. V; (b) x vs. V
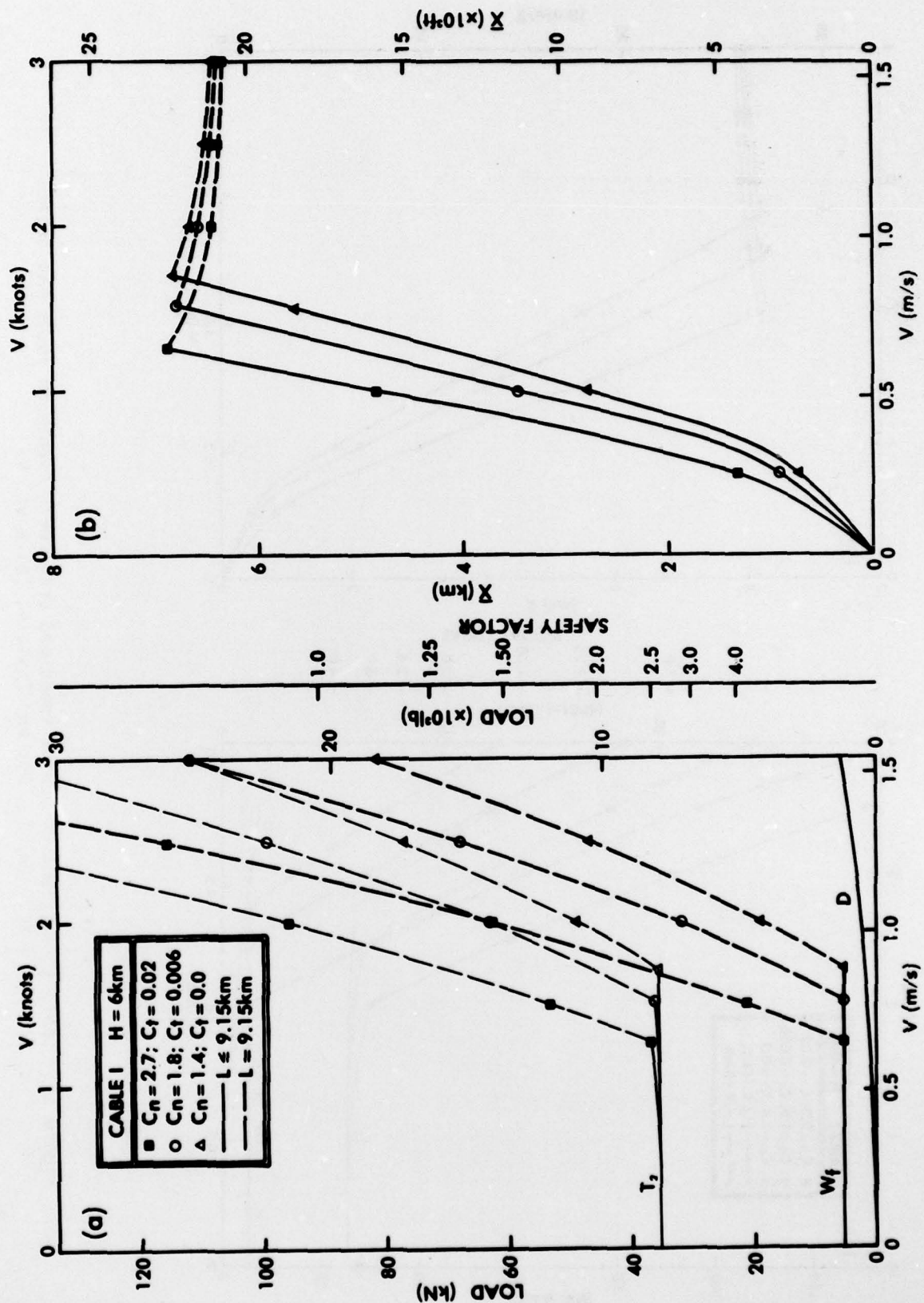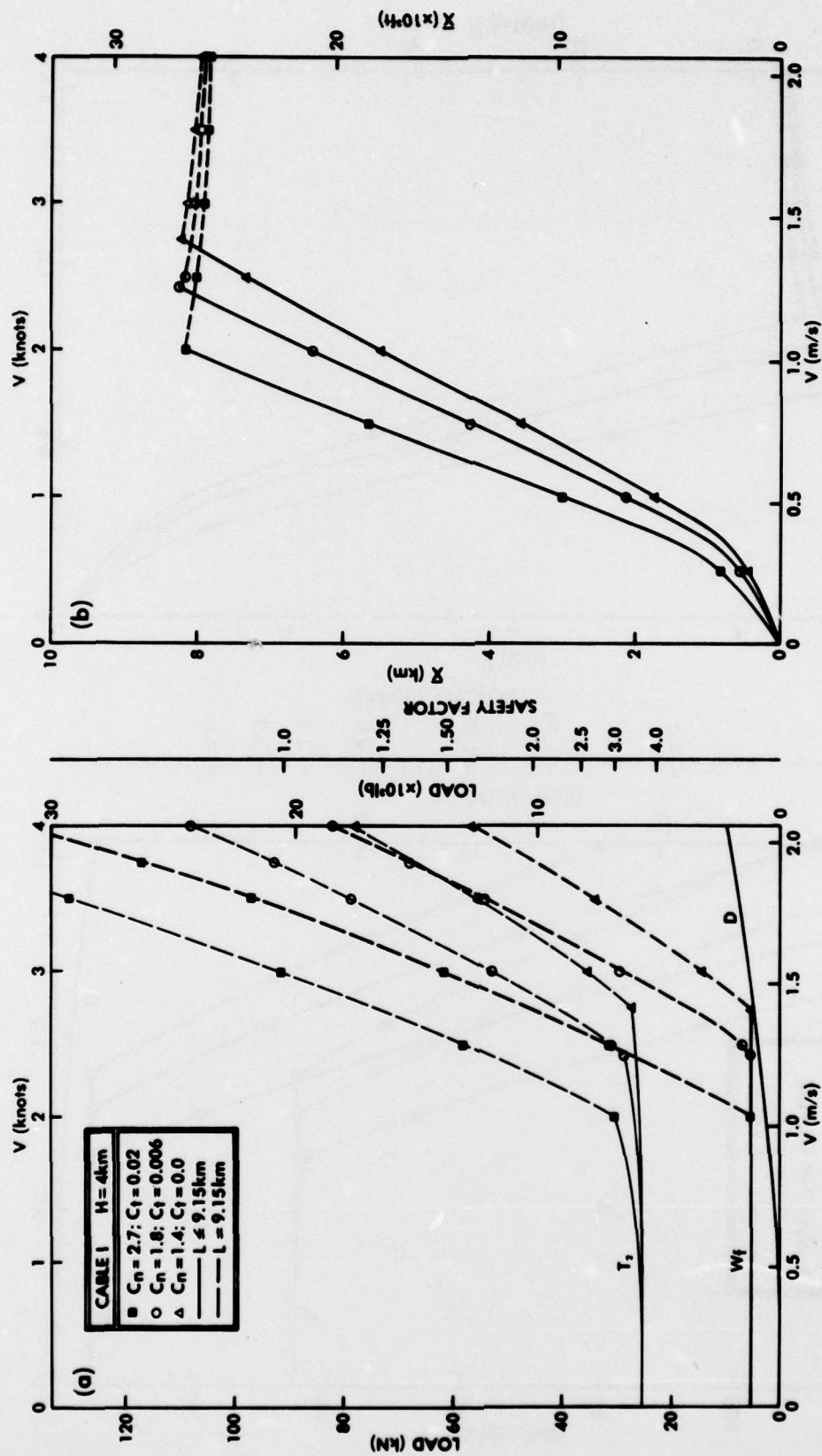
21

Figure 11. Cable I -- Effect of towing speed and drag coefficients on loads and trail for H = 4 km: (a) T_2, W_f, and D vs. V; (b) $\bar{X}$ vs. V

Figure 12. Cable II -- Effect of towing speed and drag coefficients on loads and trail for H = 6 km: (a) T_2, W_f, and D vs. V; (b) $\bar{x}$ vs. V

23

Figure 13. Cable II -- Effect of towing speed and drag coefficients on loads and trail for H = 4 km: (a) T_2, W_f, and D vs. V; (b) $\bar{X}$ vs. V.
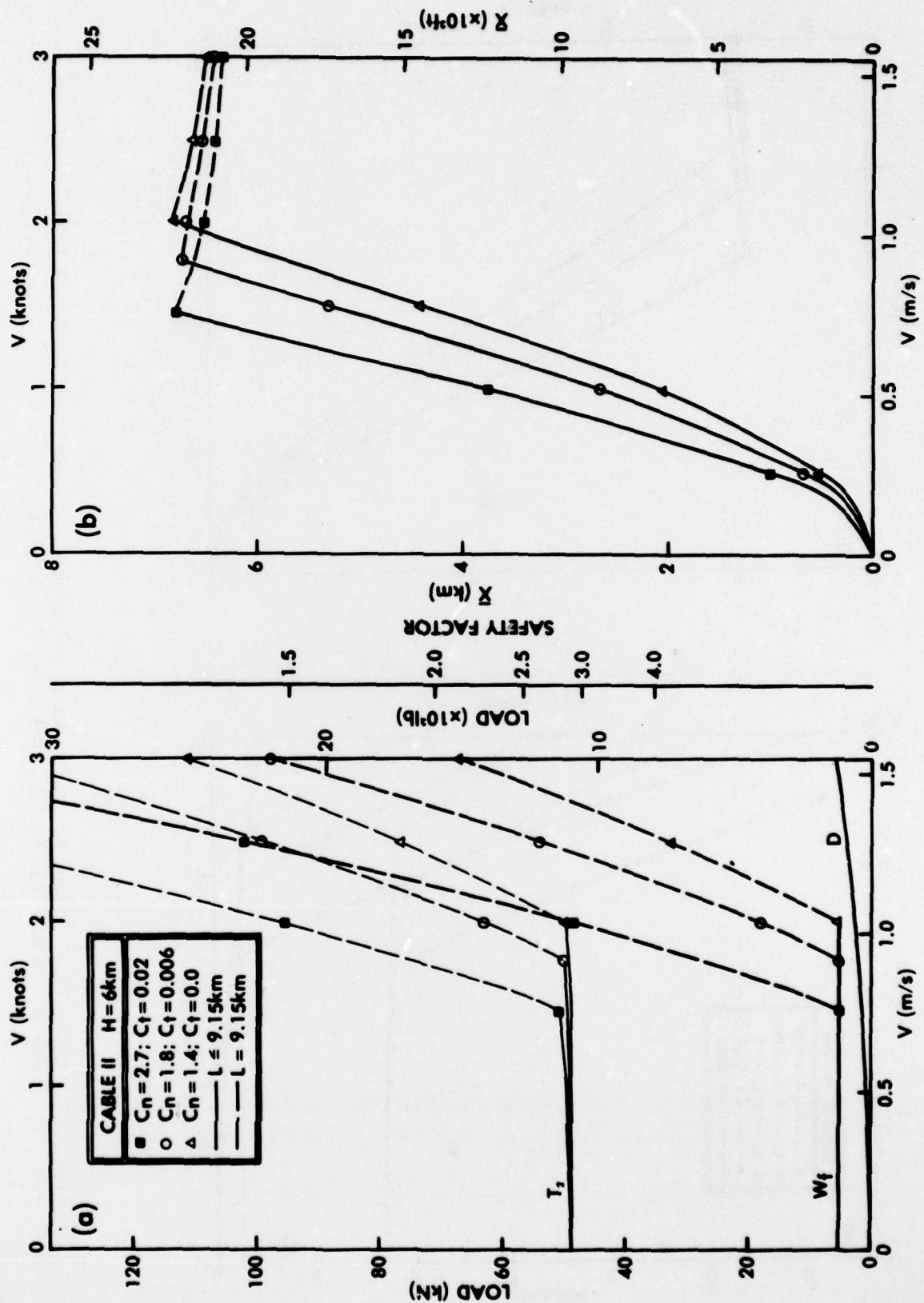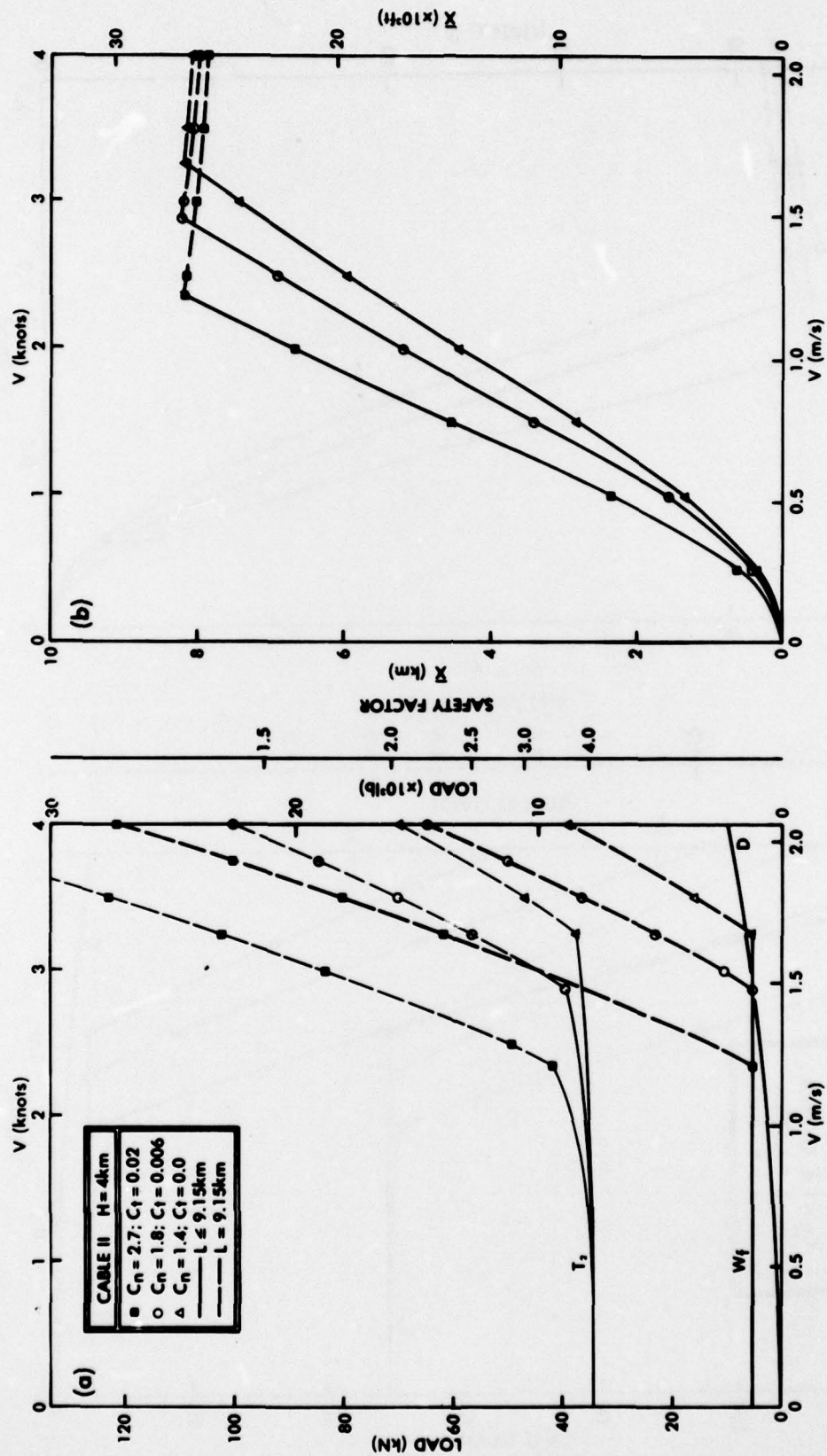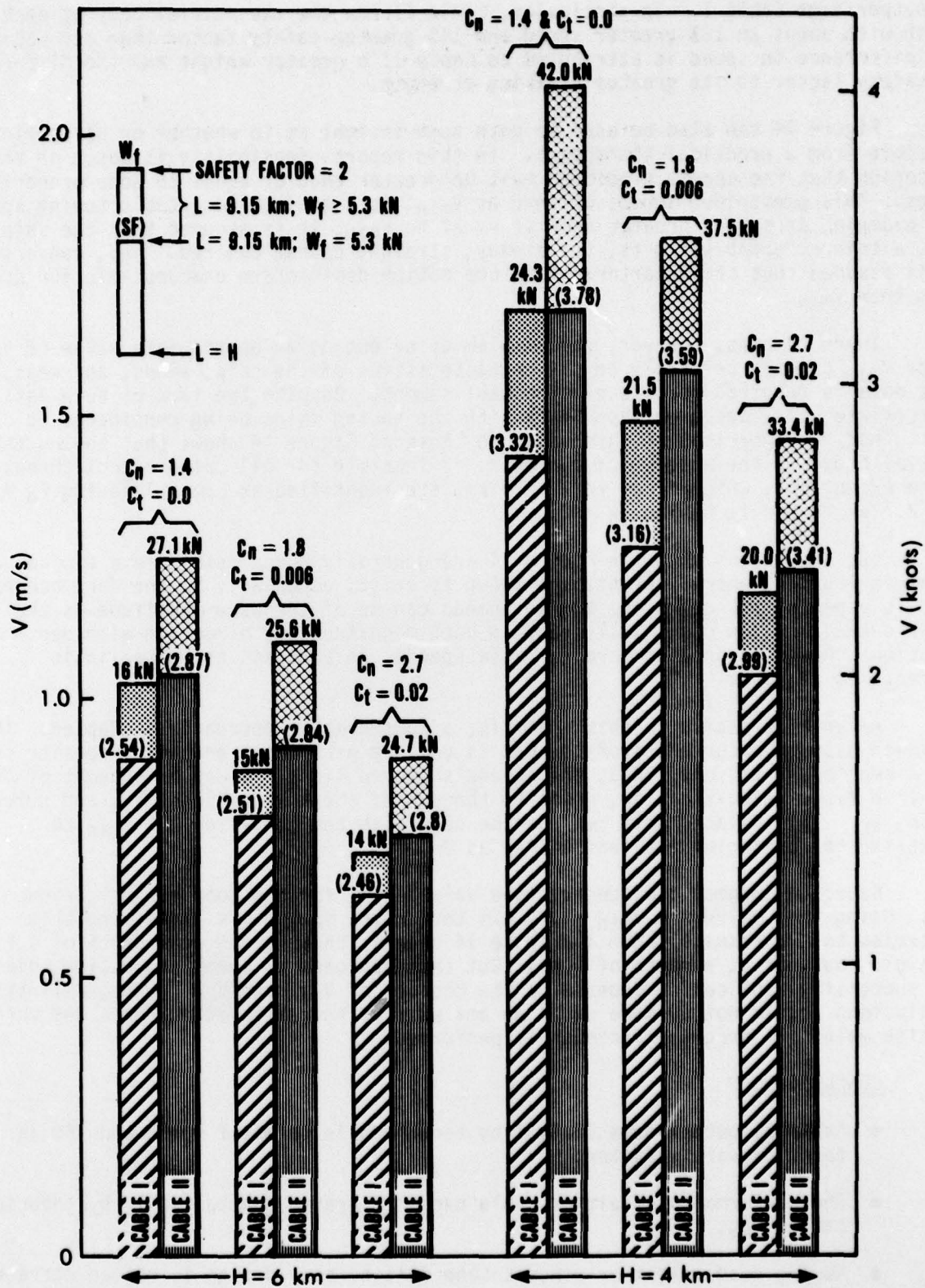
Figure 14. Performance of the candidate towing cables

II outperforms Cable I. In particular, Cable II can tow the initial body at each depth with about an 18% greater speed and 14% greater safety factor than can Cable I. The difference in speed is attributed to Cable II's greater weight and the difference in safety factor to its greater breaking strength.

Figure 14 can also be used to gain some insight as to whether or not towing is feasible from a practical standpoint. In this report, feasibility is based on the criterion that the speeds predicted must be greater than or equal to some prescribed speed. This prescribed speed, defined as V_{min}, is a minimum acceptable towing speed. For example, at speeds greater than or equal to V_{min}, it is assumed that the ship can tow, within acceptable limits, the steady, straight course desired. And, conversely, it is assumed that the departures from the motion desired are unacceptable for speeds less than V_{min}.

There remains, however, the problem of selecting an appropriate value of V_{min}. Since V_{min} depends primarily on the characteristics of the ship, winds, and seas, test data is required for its exact establishment. Despite the lack of such data, an appropriate value based on experience with the towing ships being considered is 3/4 m/s. Thus, a comparison of this value to those of Figure 14 shows that towing the initial body, in the absence of currents, is feasible for all cases except three. These exceptions, which occur for H = 6 km, are identified as Cable I having C_n = 1.8 and 2.7 and Cable II having C_n = 2.7.

But the speeds shown in Figure 14 are generally not possible in a typical ocean environment where currents are known to exist, especially in the deep ocean. This is especially true, since towing speeds can be of the same magnitude as the ocean currents which continually vary in both magnitude and direction with depth and location. Hence to predict more reliable speeds, an analysis using realistic currents is required.

As an alternative to this analysis, a conservative approach is adapted. This approach assumes a current profile that is uniform with depth and acts opposite to the direction of motion. Thus, the speeds shown in Figure 14 can be thought of as relative fluid velocities, V_R, equal to the sum of the towing speed, V_T, and current speed, V_C. This relationship can then be used with the condition $V_T \geq V_{min}$ to establish the criterion for feasibility as $V_R \geq V_{min} + V_C$.

Based on judgment, a conservative value of V_C for the deep ocean is about 1/4 m/s. Using this value and V_{min} = 3/4 m/s then gives $V_R \geq 1$ m/s. Applying this criterion to the results shown in Figure 14 reveals that towing at a depth of 4 km is feasible, but not at a depth of 6 km. But this approach is open to question, since its successful application depends on the choices of V_{min} and V_C. Hence, definite conclusions should not be made until an analysis using realistic currents and more precise values of drag coefficients is performed.

VI. CONCLUSIONS

- Cable II outperforms Cable I by about 20% in terms of speed and 14% in terms of safety factor.

- The performance of either cable can be improved substantially by reducing cable drag.

- Adding dead-weight or wings to the initial body design is not an attractive design consideration.

● The geophysical array can be towed at reasonable speeds at a depth of 4 km with either towing cable. However, at a depth of 6 km, this statement may not be true.

VII. RECOMMENDATIONS

To further aid in the design of the geophysical array system, the following work is recommended:

● Investigate the use of cable fairings.

● Examine the design features of the seismic streamer that can adversely affect deformations in the acoustic aperture. One such feature concerns the trimming of the streamer, which generally will have varying degrees of buoyancy along its length. If the locations of the depth controllers or floats used to trim the streamer are specified, then each section of streamer between controllers or floats is a separate, two-dimensional boundary-value problem. Therefore, the forces which must be exerted on the streamer by the controllers or floats, as well as the displacement of the hydrophones, can be determined using the solution technique described in Section IV-B of this report.

● Using a steady-state analysis that considers cable stretch, compute the towed system cable configurations and tensions in the presence of typical ocean currents. The results obtained from this analysis should provide useful information on the effects of cross-currents, as well as a more realistic assessment of maximum towing speeds.

● Using a dynamic analysis, investigate the tensions and motions in the towed system caused by winds, waves, and ocean currents. Specific topics addressed in this investigation should include: the motions of a candidate towing ship; the dynamic tensions of the towing cable at the ship and at the body towpoint; the motions of the seismic streamer and fish; and configuration changes of the seismic streamer due to speed change maneuvers of the ship.

● Investigate the feasibility of measuring array deformations with engineering sensors.

VIII. REFERENCES

Casarella, M.J. and M.G. Parsons (1970). A Survey of Investigations on the Configuration and Motion of Cable Systems Under Hydrodynamic Loading. MTS J., v. 4, July-August, p. 27-44.

Fagot, M.G. and B.C. Eckstein (1979). Deep Towed Geophysical Array Development, Program-Progress Report (FY 1978). Naval Ocean Research and Development Activity, NSTL Station, MS, NORDA Tech. Note 41.

Griffin, O.M. et al. (1975). The Resonant, Vortex-Excited Vibrations of Structures and Cable Systems. Offshore Technology Conference Paper, OTC 2319.

Hoerner, S.F. (1965). Fluid Dynamic Drag. Brick Town, NJ, Published by author.

Milburn, D.A. and R.R. Rumpf (1979). VEKA I: Design, Fabrication and Sea Test. Naval Ocean Research and Development Activity, NSTL Station, MS (in preparation).

Pattison, J.H. et al. (1977). Handbook on Hydrodynamic Characteristics of Moored Array Components. David W. Taylor Naval Ship Research and Development Center, Carderock, MD, Report No. SPD-745-01.

Skop, R.A. et al. (1976). Seacon II Strumming Predictions. Naval Research Laboratory, Washington, D.C., NRL Memo. Rpt. 3383, 18 p.

Wilson, B.W. (1960). Characteristics of Anchor Cables in Uniform Ocean Currents. Texas A&M University, College Station, TX, Apr., Tech. Rpt. No. 204-1, 157 p.

REPORT DOCUMENTATION PAGE		READ INSTRUCTIONS BEFORE COMPLETING FORM
1. REPORT NUMBER NORDA Technical Note 40	2. GOVT ACCESSION NO.	3. RECIPIENT'S CATALOG NUMBER
4. TITLE (and Subtitle) A Steady-state Analysis of Candidate Tow Cables for a Deep-Towed Geophysical Array System		5. TYPE OF REPORT & PERIOD COVERED
		6. PERFORMING ORG. REPORT NUMBER
7. AUTHOR(s) Darrell A. Milburn Martin G. Fagot		8. CONTRACT OR GRANT NUMBER(s)
9. PERFORMING ORGANIZATION NAME AND ADDRESS Naval Ocean Research and Development Activity NSTL Station, Mississippi 39529		10. PROGRAM ELEMENT, PROJECT, TASK AREA & WORK UNIT NUMBERS
11. CONTROLLING OFFICE NAME AND ADDRESS Naval Ocean Research and Development Activity NSTL Station, Mississippi 39529 (Code 350)		12. REPORT DATE March 1979
		13. NUMBER OF PAGES 28
14. MONITORING AGENCY NAME & ADDRESS(if different from Controlling Office)		15. SECURITY CLASS. (of this report) Unclassified
		15a. DECLASSIFICATION/DOWNGRADING SCHEDULE
16. DISTRIBUTION STATEMENT (of this Report) Unlimited		

DISTRIBUTION STATEMENT A
Approved for public release;
Distribution Unlimited

17. DISTRIBUTION STATEMENT (of the abstract entered in Block 20, if different from Report)
18. SUPPLEMENTARY NOTES
19. KEY WORDS (Continue on reverse side if necessary and identify by block number)

20. ABSTRACT (Continue on reverse side if necessary and identify by block number)

The relative performance of two candidate towing cables for the proposed Deep-Towed Geophysical Array System is examined. A preliminary design of this ship-towed system is presented. It includes a description of the candidate towing cables and a towed body, which is composed of an instrumented fish and a long, nearly neutrally buoyant seismic streamer.

Using a two-dimensional steady-state analysis, towing cable geometry and tensions are predicted for the body depths specified and for a series of towing speeds. Results of the

DD FORM 1473   EDITION OF 1 NOV 65 IS OBSOLETE
1 JAN 73   S/N 0102-014-6601 |

analysis are presented graphically and show not only the effects of body depth and towing speed, but the effects of cable drag coefficients and body downforce as well. These results are then used in conjunction with constraints on cable length and design tension to predict maximum towing speeds.

Although based on a particular design, the information contained in this report provides useful guidance to further assist in the engineering development of the overall system.